

Systematic study of insulator-metal transitions in perovskites $R\text{NiO}_3$ ($R = \text{Pr}, \text{Nd}, \text{Sm}, \text{Eu}$) due to closing of charge-transfer gap

J. B. Torrance, P. Lacorre,* and A. I. Nazzari

IBM Research Division, Almaden Research Center, 650 Harry Road, San Jose, California 95120-6099

E. J. Ansaldo

Physics Department, University of Saskatchewan, Saskatoon, Canada S7N 0W0

Ch. Niedermayer

Fakultät für Physik, Universität Konstanz, 7750 Constance, Germany

(Received 16 December 1991)

The detailed behavior of the phase transitions was mapped out for the series $R\text{NiO}_3$ as a function of the rare earth (R). A sharp insulator-metal transition is observed, which depends strongly on R . For small R it occurs at a higher temperature than the antiferromagnetic ordering (measured by muon-spin relaxation). By increasing either the temperature or the size of R , an insulator-metal transition is observed, most probably caused by the closing of the charge-transfer gap, induced by an increase in the electronic bandwidth.

The discovery of superconductivity at high temperatures in a number of oxides¹⁻³ has caused a revival of interest in oxides in general. Before the discovery of superconductivity in these materials, perhaps their most interesting property was the insulator-metal transition⁴⁻⁸ as exhibited by Ti_2O_3 , V_2O_3 , and VO_2 , for example. Theoretical discussions of these transitions were generally based on the closing of the Mott-Hubbard gap which was present because of strong Coulomb correlations. Interpretation of these transitions, however, was complicated by the fact that there were simultaneous changes in the electronic, magnetic, and structural properties and it is still difficult to identify which is the cause and which is the effect. More recently, Zaanen, Sawatzky, and Allen⁹ (ZSA) have developed a general framework for oxides (as well as sulfides, chlorides, etc.), which has been recently shown¹⁰ to be able to account for the differences between metallic and insulating conductivity for a wide variety of oxides. According to the ZSA picture, there are two general types of gaps possible: the Mott-Hubbard gap due to the Coulomb correlation energy U and the charge-transfer gap associated with an energy Δ . Associated with these two types of possible gaps, there are two types of insulators: Mott insulators (where the smallest gap is associated with U) and charge-transfer insulators (where the smallest gap is associated with Δ). Accordingly, we could expect two types of insulator-metal transitions: when the Mott-Hubbard gap closes (as attributed⁴⁻⁸ to Ti_2O_3 , V_2O_3 , and VO_2); and when the charge-transfer gap closes, as we conclude in this paper happens in $R\text{NiO}_3$. In addition to introducing a new type of insulator-metal transition, this work provides solid experimental data on the electronic energies in $R\text{NiO}_3$. Such information is fundamental to the assumptions underlying theoretical models for oxides, which should perhaps first concentrate on understanding such basic transitions before attempting to explain the relatively subtle mechanism of high-temperature superconductivity.

Metallic conductivity was observed¹¹ in LaNiO_3 , whereas LuNiO_3 and YNiO_3 appeared¹² insulating based on magnetic susceptibility measurements, which suggested antiferromagnetic ordering at $T_N = 130$ and 145 K, respectively. Very recently, insulator-metal transitions were discovered in the Sm,¹³ Nd,^{13,14} and Pr (Ref. 13) compounds, as shown in Fig. 1(a), in which the transition temperature strongly decreased with increasing size of the rare-earth ion. Associated with this insulator-metal transition, a small discontinuous decrease in the unit-cell volume is observed^{13,15} and shown in Fig. 1(b). This contraction has been attributed¹⁵ to the onset of electronic delocalization in the metallic state. In the case of the Pr and Nd compounds, the Ni spins are observed to be magnetically ordered¹³ at low temperatures, with an unusual antiferromagnetic structure,¹⁶ which disappears at the insulator-metal transition. In this paper, we report a systematic study of the insulator-metal and magnetic-phase transitions in the $R\text{NiO}_3$ series, including new data for the Eu and Sm compounds as well as for some solid solutions between those of Sm, Nd, Pr, and La, in order to map out the behavior of these phase transitions, so that we can better understand their inter-relationships and physical origins.

The difficulty of preparing¹²⁻¹⁴ compounds in the series $R\text{NiO}_3$ increases severely as the radius of the rare earth decreases. We finally succeeded in preparing ceramic pellets of EuNiO_3 by reacting the oxides at 1000 °C under an oxygen pressure of 200 bars for 3 days. The solid solutions $\text{Sm}_{1-x}\text{Nd}_x\text{NiO}_3$ and $\text{Nd}_{1-x}\text{La}_x\text{NiO}_3$ were readily prepared from the corresponding oxides (under usual conditions¹³) and exhibited the expected smooth variation of their lattice constants. We have found that differential scanning calorimetry (DSC) can be used to measure the insulator-metal transition and is more convenient for transitions above room temperature. The transition temperatures¹⁷ determined from the endothermic DSC peak corresponded well with those from resistivity measurements.

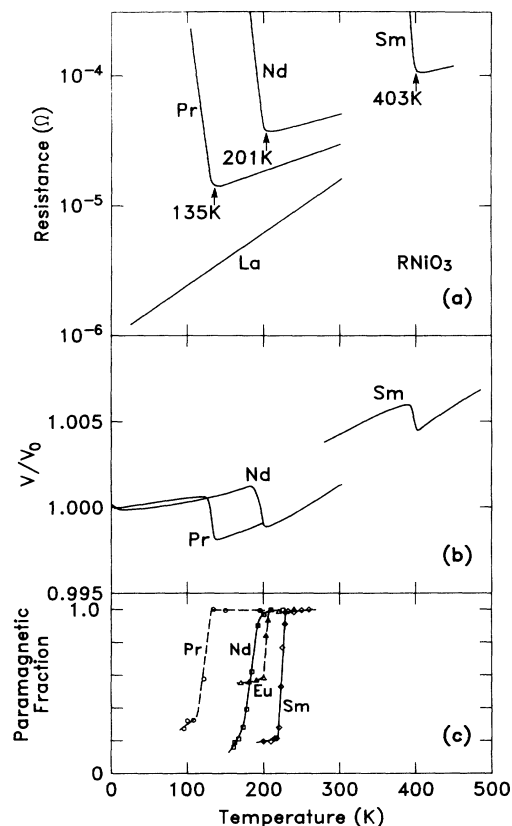


FIG. 1. (a) The resistivity of La-, Pr-, Nd-, and SmNiO₃ showing their insulator-metal transitions [after Lacorre *et al.* (Ref. 13)]; (b) the temperature dependence of the unit-cell volume for Pr-, Nd-, and SmNiO₃ showing the extra contraction occurring upon entering the metallic state [after Garcia-Muñoz *et al.* (Ref. 15)]; and (c) the paramagnetic fraction as determined from muon ⁺-spin-rotation experiments, which drops suddenly at the antiferromagnetic ordering temperature.

In order to study the relation between the magnetic-ordering temperatures and the insulator-metal transition, we have carried out positive muon-spin relaxation (μ^+ SR) experiments at TRIUMF on several members of this series. From these experiments, one can determine¹⁸ the volume fraction of the sample that is paramagnetic, which is shown as a function of temperature in Fig. 1(c) for the Pr, Nd, Sm, and Eu compounds. (The large background for EuNiO₃ occurred because the small sample allowed $\sim 40\%$ of the muon beam to be stopped in the substrate.) Similar data are obtained for the solid solutions. The initial drop in the paramagnetic fraction measures the antiferromagnetic ordering temperature, T_N . The temperatures¹⁷ (135 and 195 K) found for the Pr and Nd compounds are in excellent agreement with those from conductivity¹³ and neutron measurements of the change in lattice constants.^{13,15} In sharp contrast, the antiferromagnetic transition temperatures (225 and 205 K) found for the Sm and Eu compounds are dramatically lower than those found (at 400 and 480 K) for their respective insulator-metal transitions.

The general phase diagram for the series RNiO₃ is

shown in Fig. 2, where the observed transition temperatures are plotted as a function of the tolerance factor, t , where $t \equiv (d_{R-O})/\sqrt{2}(d_{Ni-O})$. As discussed below, the variation of t in Fig. 2 for the series RNiO₃ is caused by changes in the size of the rare-earth ion: increasing size gives rise to increasing t . Concentrating first on the conductivity behavior, the insulator-metal transition temperatures found by Lacorre *et al.*¹³ are shown as large open squares in Fig. 2, along with the data point (large triangle) for metallic¹¹ LaNiO₃. The data reported here for EuNiO₃ and the solid solutions Sm_{1-x}Nd_xNiO₃ and Nd_{1-x}La_xNiO₃ are plotted as the large open circles in Fig. 2. The data for the solid solution Pr_{1-x}La_xNiO₃ (not shown) fall near the same curve. The magnetic transitions from μ^+ SR measurements are also plotted in Fig. 2 as the small solid circles, together with earlier^{12,13} data.

It is evident from Fig. 2 that the transitions observed in RNiO₃ form a coherent pattern as a function of the tolerance factor (t). These transitions separate three distinct regimes: an antiferromagnetic insulator, a paramagnetic insulator, and a metal. These three regimes of this materials system are all found in SmNiO₃, for example. At room temperature, it is a paramagnetic insulator, but loses its paramagnetism below 225 K [Fig. 1(c)] as it enters the antiferromagnetic phase.¹⁹ Above 400 K it loses its insulating character [Fig. 1(a)] as it crosses the insulator-metal transition into the metallic phase. At low temperatures, the Ni spins in NdNiO₃ (and PrNiO₃) are also antiferromagnetically ordered, but with increasing temperature this order disappears before the expected T_N because the electrons become delocalized at the (low) insulator-metal transition. The insulating and metallic regimes in Fig. 2 are separated by a well-defined boundary or transition, the temperature of which decreases almost linearly with t (or rare-earth radius). On the other hand, the magnetic-phase boundary rises as t increases, until it reaches the insulator-metal transition, beyond which the antiferromagnetic order appears not to persist.

The GdFeO₃ structure of the RNiO₃ compounds^{12,13} is shown schematically in the inset of Fig. 2. Regular NiO₆

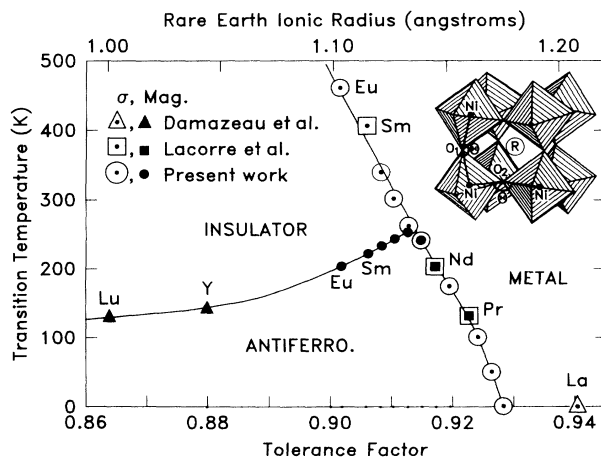


FIG. 2. Insulator-metal-antiferromagnetic phase diagram for RNiO₃ as a function of the tolerance factor and (equivalently) the ionic radius of the rare earth (R).

octahedra share corners to form a three-dimensional array, with the R ions occupying the space in between these octahedra. For our purposes, the most important feature of this structure is the Ni-O-Ni bond angle, θ , since the electronic bandwidth and the magnetic exchange interaction are closely related²⁰ to $\cos\theta$. This angle is generally less than 180° because of the orthorhombic distortion, which is conventionally discussed^{4,21,22} in terms of the tolerance factor, t , defined above. If the rare-earth ion were large enough to give $t=1$, the rare-earth-oxygen bond lengths (d_{R-O}) and nickel-oxygen bond lengths (d_{Ni-O}) would be compatible with the ideal cubic perovskite structure, i.e., the structure in Fig. 2 with no distortion and with the Ni-O-Ni bond angle $\theta=180^\circ$. Since the rare earths are too small to satisfy this criterion, the structure becomes distorted as the NiO_6 octahedra tilt and rotate in order to fill the extra space otherwise present around the rare-earth ion.

Examining the series $RNiO_3$ in Fig. 2, as the size of the rare earth and hence the tolerance factor (t) increase, the orthorhombic distortion decreases.²³ At the same time the bent Ni-O-Ni bond angle θ gradually straightens out. Quantitatively, as the rare-earth size increases from Ho (Ref. 12) ($t=0.880$) to Sm (Ref. 13) ($t=0.906$) to Pr (Ref. 13) ($t=0.923$) to La (Ref. 15) ($t=0.940$), the Ni-O-Ni bond angle increases gradually from 151.7 to 152.6° to 158.7° to 165.2° . In addition, as the temperature is increased, this angle also tends to straighten out (probably driven by entropy). This effect has been measured in the case of $PrNiO_3$ by Huang *et al.*,²⁴ who found that θ increases by $\sim 1.5^\circ$ between 300 and 673 K. It should be emphasized that the behavior of θ as a function of t and T is a general, steric feature of these structures and is also present in other distorted perovskite systems,²⁵ for example, $RAIO_3$. In these structures, increasing t and/or T also increases the $M-O-M$ angle, for $M=Al, Fe$, etc.

This gradual variation in θ over the space of Fig. 2 is not significantly complicated by structural changes occurring at the insulator-metal transition. A careful neutron structure examination^{13,15} of this transition in $PrNiO_3$ and $NdNiO_3$ found *no* change in lattice symmetry and no evidence of superlattices. Hence, the only structural change at the transition appears to be the very small ($\sim 0.2\%$) change in unit cell volume, which can be quantitatively accounted for¹⁵ by a decrease in the Ni-O bond length of 0.0035 \AA , presumably induced by electronic delocalization ("metallic bonding"). These small changes are in contrast with the larger ones found in the widely studied⁴⁻⁸ V_2O_3 system, where there is a 3.5% change in volume at the insulator-metal transition and a change in lattice symmetry from monoclinic to trigonal. This latter insulator-metal transition is thus complicated by the significant role played by structural changes in driving the transition. In contrast, in the $RNiO_3$ series, there are only relatively small changes in unit-cell volume, which are induced by the insulator-metal transition.

The space spanned in Fig. 2 thus contains a range of tolerance factor and temperature over which there is a gradual and continuous variation of θ and hence of the electronic bandwidth: an ideal system for systematic studies of electronic properties. The general behavior of

the $RNiO_3$ compounds in Fig. 2 can be reasonably understood as follows: as the tolerance factor and/or the temperature increase, the bandwidth increases and the compounds become more metallic. In fact, they become more metallic at an abrupt insulator-metal phase transition. The magnetic-ordering temperature is also expected to increase as the bandwidth increases: hence its rise with increasing tolerance factor in Fig. 2.

As mentioned in the introduction, corresponding to the two types of insulators in the ZSA framework⁹ (Mott-Hubbard and charge-transfer), there are expected to be two types of insulator-metal transitions. The identification of the physical mechanism of the transition in the $RNiO_3$ system is taken from a broad study¹⁰ of transition-metal oxides that uses the ZSA framework and a simple ionic model in order to estimate the relevant energies. In this comparison of 76 oxide compounds, there appear boundaries which separate the insulators from the metals. Furthermore, it identifies Ti_2O_3 , V_2O_3 , and $RTiO_3$ (which each have an insulator-metal transition) as lying near the boundary between metals and insulators with small Coulomb correlation (U) gaps, in agreement with the traditional interpretation.⁴⁻⁸ The two systems VO_2 and $RNiO_3$, however, are shown¹⁰ to lie near the insulator-metal boundary where the charge-transfer gaps are small.

Our model for $RNiO_3$ is thus shown schematically in Fig. 3. For small rare earths, the structure contains bent Ni-O-Ni bonds, a lower bandwidth, and is insulating. The gap is a charge-transfer gap between the occupied oxygen $2p$ valence band and the unoccupied Ni $3d$ conduction band. The insulating ground state may be crudely viewed as ionic, containing O^{2-} and Ni^{3+} ions, with Ni^{3+} in a low-spin state.¹⁶ As the bandwidth is increased, the charge-transfer gap decreases, eventually going to zero, as the valence and conduction bands overlap, giving rise to a semimetallic state. In this low- Δ metal, the concept of ionic Ni^{3+} and O^{2-} loses its meaning, as unpaired electrons occur on both types of sites. The fact that the bandwidth may be increased by either increasing the temperature or the rare-earth size gives rise to the phase boundary in Fig. 2. The data for small rare earths show separate

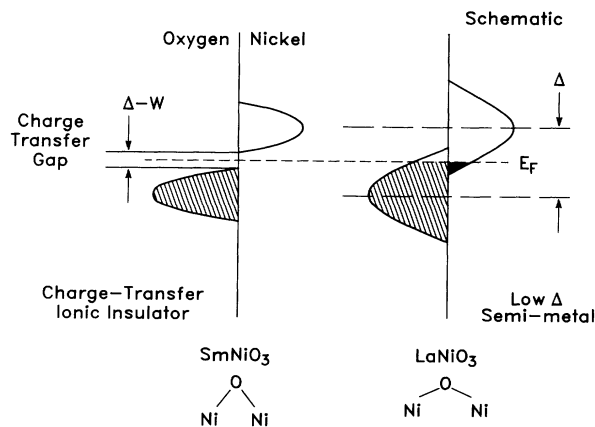


FIG. 3. Schematic diagram of model for insulating and metallic phases of $RNiO_3$.

magnetic and electronic transitions, allowing us to separate the roles of the different effects.

Finally, we note that suggestions²⁶ that low-energy charge-transfer excitations might give rise to high-temperature superconductivity make the anomalously low- Δ system $RNiO_3$ especially attractive for further study.

Research at TRIUMF is supported by the Natural Sciences and Engineering Research Council of Canada and,

through TRIUMF, by the Canadian National Research Council. We wish to thank Rich Siemens for the DSC measurements, and C. E. Stronach, M. Davies, R. S. Carey, and G. D. Morris for helping with the μ^+ SR measurements, as well as J. Pannetier and J. Rodríguez-Carvajal for fruitful discussions. In addition, J.B.T. would like to gratefully acknowledge the Spanish Ministry of Education for hospitality and financial support while some of this work was performed.

*Permanent address: Lab des Fluorures, Faculté des Sciences, Université du Maine, 72017 LeMans, CEDEX, France.

¹A. W. Sleight, J. L. Gillson, and P. E. Bierstedt, *Solid State Commun.* **17**, 25 (1975).

²J. G. Bednorz and K. A. Müller, *Z. Phys. B* **64**, 189 (1986).

³R. J. Cava, B. Batlogg, J. J. Krajewski, R. Farrow, and L. W. Rupp, *Nature (London)* **332**, 814 (1988).

⁴J. B. Goodenough, *Prog. Solid State Chem.* **5**, 149 (1971).

⁵D. Adler, *Radiat. Eff.* **4**, 123 (1970), and references therein.

⁶N. F. Mott, *Metal-Insulator Transitions* (Taylor and Francis, London, 1974).

⁷D. B. McWhan, J. P. Remeika, T. M. Rice, W. F. Brinkman, J. Maita, and A. Menth, *Phys. Rev. Lett.* **27**, 941 (1971); *Phys. Rev. B* **5**, 2252 (1972).

⁸M. Yethiraj, *J. Solid State Chem.* **88**, 53 (1990), and references therein.

⁹J. Zaanen, G. A. Sawatzky, and J. W. Allen, *Phys. Rev. Lett.* **55**, 418 (1985); J. Zaanen and G. A. Sawatzky, *J. Solid State Chem.* **88**, 8 (1990).

¹⁰J. B. Torrance, P. Lacorre, C. Asavaroengchai, and R. M. Metzger, *J. Solid State Chem.* **90**, 168 (1991); *Physica C* **182**, 351 (1991); J. B. Torrance, *J. Solid State Chem.* **96**, 59 (1992).

¹¹J. B. Goodenough and P. M. Raccach, *J. Appl. Phys.* **36**, 1031 (1965); A. Wold, B. Post, and E. Banks, *J. Amer. Chem. Soc.* **79**, 4911 (1957).

¹²G. Demazeau, A. Marbeuf, M. Pouchard, and P. Hagenmuller, *J. Solid State Chem.* **3**, 582 (1971).

¹³P. Lacorre, J. B. Torrance, J. Pannetier, A. I. Nazzal, P. W. Wang, and T. C. Huang, *J. Solid State Chem.* **91**, 225 (1991).

¹⁴J. K. Vassiliou, M. Hornbostel, R. Ziebarth, and F. J. DiSalvo, *J. Solid State Chem.* **81**, 208 (1989).

¹⁵J. L. Garcia-Muñoz, J. Rodríguez-Carvajal, P. Lacorre, and J. B. Torrance (unpublished).

¹⁶J. L. Garcia-Muñoz, J. Rodríguez-Carvajal, and P. Lacorre (unpublished).

¹⁷The transitions are weakly first order, with a "width" apparent in x-ray measurements and a small hysteresis observed in conductivity.

¹⁸The paramagnetic fraction is determined from experiments performed in a weak external field ($H \lesssim 100$ Oe) applied transverse to the initial polarization direction. See, for example, Y. J. Uemura *et al.*, *Phys. Rev. Lett.* **59**, 1045 (1987); J. H. Brewer *et al.*, *ibid.* **60**, 1073 (1988).

¹⁹It is not known if all compounds in the antiferromagnetic regime have the same unusual magnetic structure as found for the Nd and Pr compounds. (See Ref. 16.)

²⁰See, for example, G. A. Sawatzky, W. Geertsma, and C. Haas, *J. Magn. Magn. Mater.* **3**, 37 (1976).

²¹V. M. Goldschmidt, *Skr. Nor. Vidensk. Akad. Mat. Naturvidensk. Kl.* **2**, 1 (1926).

²²For the tolerance factor, we used $d_{Ni-O} = 1.94$ Å and the values for d_{R-O} for coordination number of 8 from P. Poix, *C. R. Acad. Sci. (Paris)* **270C**, 1852 (1970).

²³For still larger values of t , there is a phase transition to a rhombohedral phase, but this transition is well separated from the transitions in Fig. 2.

²⁴T. C. Huang, W. Parrish, H. Toraya, P. Lacorre, and J. B. Torrance, *Mater. Res. Bull.* **25**, 1091 (1990).

²⁵See, for example, M. Marezio, J. P. Remeika, and P. D. Dernier, *Acta Crystallogr. Sect. B* **26**, 2008 (1970).

²⁶W. A. Little, *J. Phys. (Paris) Colloq.* **44**, C3-819 (1983); C. M. Varma, S. Schmitt-Rink, and E. Abrahams, *Solid State Commun.* **62**, 681 (1987).